Theoretical Investigations of Geometry, Electronic Structure and Stability of UO6: Octahedral Uranium Hexoxide and Its Isomers

ARTICLE *in* THE JOURNAL OF PHYSICAL CHEMISTRY A · AUGUST 2010

Impact Factor: 2.69 · DOI: 10.1021/jp102107n · Source: PubMed

4 AUTHORS, INCLUDING:

Hai Xiao
California Institute of Technology
13 PUBLICATIONS **230** CITATIONS

SEE PROFILE

W H Eugen Schwarz
Universität Siegen
199 PUBLICATIONS **3,838** CITATIONS

SEE PROFILE

Jun Li
Tsinghua University
283 PUBLICATIONS **8,860** CITATIONS

SEE PROFILE

Theoretical Investigations of Geometry, Electronic Structure and Stability of UO_6: Octahedral Uranium Hexoxide and Its Isomers[†]

Hai Xiao, Han-Shi Hu, W. H. Eugen Schwarz,[‡] and Jun Li*

Department of Chemistry & Key Laboratory of Organic Optoelectronics and Molecular Engineering of the Ministry of Education, Tsinghua University, Beijing 100084, China

Received: March 8, 2010; Revised Manuscript Received: May 31, 2010

The existence of a novel octahedral UO_6 complex had been suggested by Pyykkö et al. [Pyykkö, P.; Runeberg, N.; Straka, M.; Dyall, K. G. *Chem. Phys. Lett.* **2000**, *328*, 415]. We have now investigated the stability, the geometric and electronic structures, and the vibrations of various UO_6 molecules, using spin−orbit density functional and scalar-relativistic coupled-cluster approaches. We find four different (meta-)stable species, namely $^3D_{2h}$-$UO_2(\eta^2\text{-}O_2^{\bullet})_2$ at lowest energy, $^3C_{2v}$-$UO_4^{\bullet}(\eta^2\text{-}O_2^{\bullet})$ and $^1D_3$-$U(\eta^2\text{-}O_2)_3$ at medium energies, and ^1O_h-UO_6 at highest energy. The decay of O_h-UO_6 occurs via an activated spin-flip mechanism. The UO_6 species correspond to local minima on singlet and triplet energy surfaces and might be trapped in noble gas matrices. Experimentally, the four species might be identified through their vibrational spectra. Uranium is best described as coordinated by oxygen atoms in various oxidation states as oxo O^{2-}, oxido(1) $O^{\bullet-}$, peroxido O_2^{2-}, and superoxido $O_2^{\bullet-}$ ligands. The occurrence of monovalent oxygen is remarkable. The resulting characterization of the central ion as U^{VI} in all four cases does not fully reflect the electronic differences, nor the "valence-activity" of the U-$6p^6$ semicore shell.

1. Introduction

Structure and transformation of matter are the central themes of chemistry. The duties and aims of theoretical chemistry are the computation of respective data, the physical description of the details, and the explanation in chemical terms. We will present here theoretical investigations of some new molecular species of UO_6 first investigated by Pyykkö (see below). We will here present predictions of some new molecular species of composition UO_6, describe their structure and stability, and elaborate on the chemical concepts of bonding, charge, and oxidation state, which are still under acute discussion.[1−4] Before the formulation of relevant questions at the end of this section, we will briefly review some knowledge about the formal concept of oxidation state and about oxygen ligands and uranium−oxygen compounds. This will naturally lead us to our conclusions in Section 5. The computational procedures are specified in Section 2. The octahedral UO_6 molecule is discussed in Section 3 and the three new UO_6 isomers in Section 4.

Oxidation States (OS). IUPAC[5] defines the OS as "counted according to an agreed-upon set of rules..." where the values are to be calibrated by the recipe that "oxygen has an oxidation state of −2 in most compounds". Thus, the OS is a somewhat ambiguous, formal, "nonphysical" concept, though chemically very convenient for book-keeping of chemical structures and reaction equations, and very useful for the design of new synthetic routes. Although no one-dimensional relation exists between the OS and effective atomic charges Q_{eff}, there indeed show up multivariate correlations between OS, Q_{eff}, electronegativity, several response properties, and so on.[4]

The highest oxidation states (HOS) of the chemical elements are realized in oxides and fluorides.[3a] In the first three transition rows (excluding the lanthanoid block) the HOS corresponds to the number of electrons in the valence shells, that is, to the group number in the periodic table. The HOS increases in steps of 1 from +1 for the alkali metals up to +7 for Mn (group 7) and +8 for Ru, Os and Ir (groups 8 and 9). It then decreases down to 2 in group 12 (neglecting some metastable Hg^{III} and Hg^{IV} molecules)[6] and again increases in steps of 1 toward +8 for the heavier "noble gases" of group 18. Examples for the HOS with O^{2-} ligands found so far (i.e., +8) comprise RuO_4, OsO_4, IrO_4, and XeO_4.[7,8] The XeO_4 molecule is of particular interest, since its oxygens are tetrahedrally bound through the four semicore shell pairs of Xe-$5s^25p^6$. The so far known HOS of the early actinoids, Ac^{III}, Th^{IV}, Pa^{V}, U^{VI}, Np^{VII}, and (potentially) Pu^{VIII}, fit well into this picture.[9]

As a typical "early actinoid", uranium has 6 valence-active electrons in a band of spin−orbit split $5f_{5/2,7/2}$, $6d_{3/2,5/2}$, and $7s_{1/2}$ orbitals, which lead to common OS of +3, +4, and +6, and to less common ones of +2 and +5. Remarkable structures of U^{VI} compounds have been found,[10] although no experimental indications yet for higher oxidation states, see for example ref 11, Pyykkö et al. had computationally investigated the UO_6 species already a decade ago.[12] A spectacular aspect of their work was a potential jump of the known HOS of +8 to a new record of +12, provided one attaches the common OS of −2 to the oxygens of UO_6. An OS of +12 means that the polarizable, spin−orbit split U-$6p_{3/2}^4$ and U-$6p_{1/2}^2$ semicore shells are fully included in the count of valence-active orbitals, highlighting the semivalence feature of the [Rn] noble-gas shell in uranium. However, the U-6s and U-$6p_{1/2}$ shells are relativistically stabilized, and the latter one is spin-mixed, which should hamper its valence participation.[13,14] The hypothetical dodecavalent uranium had been discussed by Hoffmann,[15] Dyall et al.,[9c] and Schulz and Liebman.[16]

[†] Part of the "Klaus Ruedenberg Festschrift".

* To whom correspondence should be addressed. E-mail: junli@tsinghua.edu.cn.

[‡] Permanent address: Theoretical Chemistry, The University, 57068 Siegen, Germany. E-mail: schwarz@chemie.uni-siegen.de.

10.1021/jp102107n
Published on Web 06/24/2010

Oxygen as a Ligand. Coordinated oxygen is known to occur in various forms as monatomic oxo or oxido(2) O^{2-} and oxido(1) $O^{\bullet 1-}$; as diatomic peroxido O_2^{2-}, superoxido $O_2^{\bullet 1-}$, and dioxygeno $O_2^{\bullet\bullet}$; and as triatomic ozonido $O_3^{\bullet 1-}$ ligands. The latter ones function as η^2-bidentate except under specific geometric conditions. The calculated (experimental)[17] O−O distances of free (bonded) O_2 species are 105.4 (106) pm for O_2^{2+}, 112.1 (112) pm for $O_2^{\bullet +}$, 121.5 (121) pm for $O_2^{\bullet\bullet}$, 135.1 (134) pm for $O_2^{\bullet -}$, and 156.9 (∼149) pm for O_2^{2-}. That is, the charge number q and bond order BO of coordinated O_2 can be estimated from the bond length (R_{OO} = 121 pm + ΔR · pm) through $q \approx 2(BO-2) \approx -0.107\ \Delta R + 0.00135\ \Delta R^2$.

Many natural and artificial uranium−oxygen coordination compounds are known,[18] comprising the peroxidic minerals studtite $UO_2(O_2)(OH_2)_4$ and metastudtite $UO_2(O_2)(OH_2)_2$.[19] Typically, up to six oxygen atoms are "equatorially" coordinated around a (nearly) linear uranyl unit with O−U−O "vertical" distances around 1.8 ± 0.1 Å, which corresponds to U≡O to U═O bonding. The equatorial U−O distances are typically in the range of 2.35 ± 0.15 Å and correspond to single dative bonds with more or less polar contributions and back-donation.[20] A specific property of the uranium−oxygen coordination seems to be the "internal clockwork like" behavior (Pyykkö)[21] of the system of cooperatively interacting U−O bonds of various bond orders and bond lengths around the central U atom.

Tetra-coordinated transition metal atoms with an empty d-valence shell prefer tetrahedral bond angles (e.g., tetrahedral OsO_4 and MnO_4^- and strongly bent $[CrO_2]^{2+}$ chromyl), whereas the actinoid metal atoms with an f-d-valence shell tend to have linear bonding such as in uranyl $[UO_2]^{2+}$.[14,22,25] Compared to the lanthanoids, the d and f shells of the actinoids are more valence active. Another specific of actinoid chemistry in comparison to transition metal chemistry is the above-mentioned valence participation of the [Rn] shell. Hoffmann had noted the synergic coupled interaction of the U-6p and O-2s semicore shells with the U-5f, U-6d, and O-2p valence shells.[25]

The UO_6 Challenge. Actinide compounds pose a particular computational and conceptual challenge because of the multitude of simultaneous problems, which could not all be accounted for simultaneously a decade ago.[12] Theses are the complex many-orbital valence shells of compact (5f, 6d) and diffuse (7s, 7p) character; the rather soft (6s, 6p) outer core shell; significant static and dynamic electron correlations; and scalar (SR) and spin−orbit (SO) relativistic effects. Pyykkö's conjecture was a high-energy octahedral $U^{XII}O_6$ spin-singlet species, found to be stable against decay into the atoms (U + 6O) and even into solid uranium and dioxygen molecules ([U] + $3O_2$). In contrast, XeO_4 is thermodynamically highly unstable against decay into Xe + $2O_2$, although still experimentally accessible. The existence of other neutral and charged UO_n^{q-} structures had also been suggested.

The noble gas shell, in particular $6p_{3/2}^4$, of the elements from radon onward including the early actinoids, is not well separated from the 5f-6d-7s valence shell. The atomic relativistic Dirac−Fock orbital energy of U-$6p_{3/2}$ is only 17 eV below U-$5f_{5/2}$, but it is nearly 7 eV *above* O-2s. Concerning the orbital radii, the U-6s, $6p_{1/2}$, and $6p_{3/2}$ semicore shells (0.8, 0.9, and 1.0 Å) lie between the U-5f inner-valence (0.76 Å) and the U-6d,7s outer-valence shells (1.7, 2.3 Å).[23] Accordingly, U-6p is easily angular-polarized by d and f hybridization and radial-relaxed upon variable 5f occupation. At short bond distances, the U-6p orbitals strongly interact with energetically adjacent ligand orbitals through orbital overlap. This causes some "6p-oxidation", that is, electron transfer to the uranium and oxygen valence shells, and leads to a rare relativistic bond-length expansion.[24] The role of the 6p shell in seventh-row compounds has often been discussed.[9c,12−15,22,25,26] X-ray spectra and nuclear quadrupole coupling constants, for instance, give experimental evidence of 6p vacancies.

On this background, we will investigate the following four points:

(i) Is ^1O_h-UO_6 a stable molecule in vacuum? Our calculations with both electron correlation and scalar and spin−orbit relativistic effects support Pyykkö's conjecture: ^1O_h-UO_6 is a weekly metastable species.

(ii) What are the possible reaction paths, activation barriers and products of the thermal decomposition of ^1O_h-UO_6? We find a spin-flip decay over a low barrier (of the order of 10−20 kcal/mol) leading to $^1D_{2d}$-UO_4 and $^3\Sigma_g^-$-O_2 with a large exothermicity of 60−70 kcal/mol.

(iii) Are there further stable or metastable isomers of UO_6? We find three new isomers, with ^1O_h-UO_6 being the energetically highest one among the four. The isomers differ geometrically and in the bonding states of the oxygens. The most stable isomer of UO_6, about 130 kcal/mol below ^1O_h-UO_6, is $^3D_{2h}$-$UO_2(O_2)_2$. It is a (structurally modified) homologue of the experimentally observed $^3C_{2v}$-$Cr^{VI}(O^{2-})_2(O_2^-)_2$.[27]

(iv) Which oxidation states should be attached to the U and O atoms in these four UO_6 molecules, and which bond orders to the U−O and the O−O interactions? According to our analyses of the wave functions, structures, and energies, uranium may be represented as U^{VI} in all four isomers. Oxygen occurs in various oxidation states, as described by low-energy di-superoxido-uranyl $^3D_{2h}$-$[U^{VI}(O^{2-})_2]^{2+}(\eta^2$-$O^{1/2-}{}_2)^{\bullet}{}_2$, by medium-energy superoxid $^3C_{2v}$-$[UO_4]^{\bullet +}(\eta^2$-$O^{1/2-}{}_2)^{\bullet}$ and triperoxid $^1D_3$-$U^{VI}(\eta^2$-$O^{1-}{}_2)_3$, and by the high-energy, high-symmetric hexoxid(1) ^1O_h-$U^{VI}(O^{1-})_6$.

2. Methodology

Choice of Hamiltonian. The SR calculations of Pyykkö et al.,[12] with or without electron correlation, yielded octahedral UO_6 as a local energy minimum, where the U-5f,6d type densities populate degenerate t_{1u}, t_{2u} and e_g type ligand molecular orbitals. However, including *spin−orbit* interactions at the noncorrelated single-reference Dirac−Fock (DF) level revealed a different lowest-energy state, with two electrons in a non-bonding MO of U-5f-a_{2u} character. This state undergoes a spin−orbit-induced distortion of the O_h structure. Pyykkö et al. had stressed that computationally very demanding simultaneous accounts of SR and SO relativistic effects and of electron correlation at the multireference (MR) level are essential for quantitative investigations, in particular concerning the possibility of *different geometric-electronic structures*.

We can now present approximate scalar plus spin−orbit relativistic calculations (SR + SO) of different geometric isomers and transition states of species of UO_6 composition. Electron correlation was approximated by various approaches based on density functional theory (DFT) within the single-determinant Kohn−Sham scheme. It is known that coordinative bonds often cause problems with single-reference methods, connected to the intermediate or low metal−ligand and ligand−ligand overlap values.[29c] Although local density functional approaches (LDA) for the exchange-correlation (XC) effects tend to be particularly effective for heavy atomic systems, they fail in cases of pronounced nondynamical correlation. In such cases, some of the generalized gradient approaches (GGA) to DFT are more successful.[27−29] Eventually, we performed

single-point coupled cluster (CC) calculations to obtain more reliable relative energies of the species.

Numerical Procedures. We have used two relativistic DFT program packages, which account simultaneously for SR and SO relativistic effects: (i) ADF, applying the relativistic zero-order regular approximation (ZORA) and the all-electron frozen atomic-core-orbital approximation;[30,31] and (ii) NWChem, using the relativistic spin-dependent effective core-potential approach.[32] In both cases, the chosen relativistic small core (RSC) comprised orbitals U-$1s_{1/2}$ through U-$4f_{7/2}$. That is, only the 32 outer-core and valence electrons of U in shells 5s to 7p were explicitly treated in the molecules.

The ADF calculations employed the LDA with Slater−Vosko−Wilk−Nusair XC functionals,[33] or the GGA with BLYP, PW91, and PBE XC functionals.[34] Uncontracted all-electron triple-ζ STO basis sets were augmented by p-functions for U, and by single d- and f-polarization functions for O (TZ2P). The basis set superposition error (BSSE) was explicitly corrected by the counterpoise recipe.[35] With analytical energy gradient techniques, the geometries were fully optimized using NR (nonrelativistic), SR, or SR + SO approaches under the proper point group symmetry. Vibrational frequencies were then calculated with high numerical precision (INTEGRATION = 8.0) to eliminate numerical noise. The absence of "imaginary" frequencies proved that the optimized structures correspond to local energy minima and not to transition states. Linear synchronous transit (LST) calculations with a fractional occupation number (FON) DFT method[36] were finally performed to evaluate the energy barriers against decay of the octahedral structure. During these calculations, the free geometric parameters were fully optimized for each value of the reaction path parameter.

The NWChem calculations were performed with the XC functionals mentioned above, and also with the hybrid-GGA functionals B3PW91, B3LYP,[37] and PBE0,[38] and with the hybrid-meta-GGA functional M06.[39] The M06−2X functional fitted for main-group compounds did not yield reasonable results for the UO_6 species (see supporting data). A Gaussian (12s11p10d8f)/[8s7p6d4f] valence basis set of triple-ζ quality was used for U,[40] which was augmented by two g-type polarization functions,[12] denoted as RSC + 2g. Dunning's aug-cc-pVTZ (AVTZ) basis set was used for O.[41] The geometries were fully optimized at the SR + SO level. We used the numerical energy gradient processing of NWChem for the calculations of the SO−DFT vibrational frequencies. Finally, single-point energy calculations of the relative stabilities of the isomers at the PW91-DFT geometries were performed at the single-reference SR CCSD(T) level.

3. Octahedral UO_6

Pyykkö et al.[12] had initiated a series of intriguing questions on UO_6, which we may extend here: (1) Taking correlation and SR+SO effects simultaneously into account, will UO_6 have O_h or distorted geometry? (2) What is the electronic U-6p core and U-5f6d valence configuration of the UO_6 ground state? (3) Will the local energy minimum of UO_6 be deep enough to render a finite lifetime possible under ambient conditions? (4) Which vibrational frequencies are characteristic for UO_6? (5) Are there further, possibly more stable UO_6 isomers than at O_h symmetry? We recall the experimentally identified $Cr^{VI}O_6$ containing also $O_2^{\delta-}$ ligands with $\delta = 0$, 1, or 2;[27] and the famous $Cr^{VI}O_5$ species with two O_2^{2-} ligands in common $CrO(\eta^2\text{-}O_2)_2$, or with one O_2^0 ligand in predicted $CrO_3(\eta^1\text{-}O_2)$.[42] (6) Can the possible isomers be discriminated by IR or Raman spectroscopy? (7) What do the geometric parameters tell us about the bonding mechanism of these novel uranium species? (8) What is a chemically reasonable interpretation of the quantum mechanical electronic structure of the molecules?

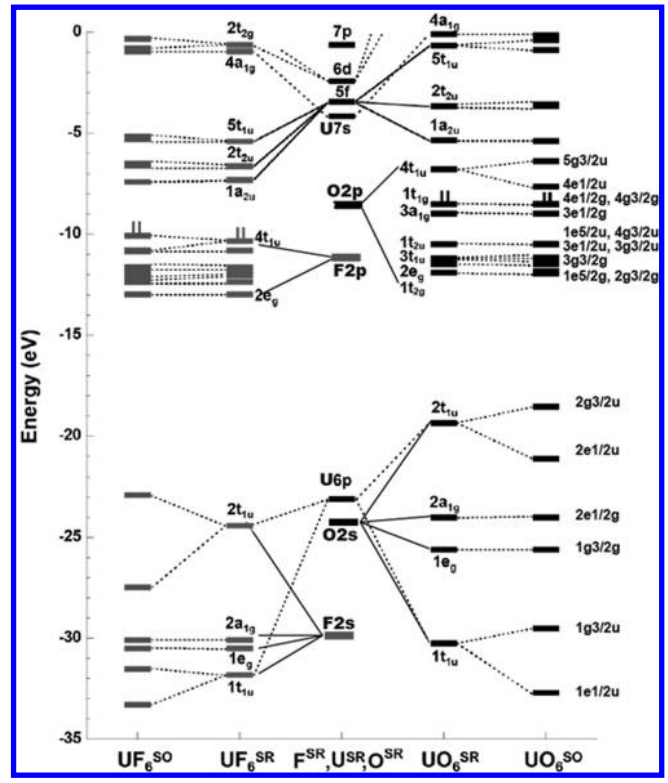

Figure 1. Relativistic Kohn−Sham orbital energy level schemes (ADF/PW91/TZ2P). Middle: Spin-averaged scalar-relativistic (SR) atomic semicore levels F-2s, O-2s and U-6p, and valence levels F-2p, O-2p and U-5f,6d,7s,7p. Left and Right: Orbital levels of O_h-UF_6 and O_h-UO_6, respectively; SR and, at the margins, SO split. The HOMOs are marked with two vertical bars.

TABLE 1: Valence orbitals of O_h-UO_6[a])

species	ϵ[b]	type		dϵ/dR[c]
		Semicore O-2s, U-6p		
$1t_{1u}$	−30.5	Os(p)-Up(f)	σ-bonding	−9.8
$1e_g$	−25.7	Os(p)-Ud	σ-bonding	−3.9
$2a_{1g}$	−24.2	Os-Us	σ-antibonding	+1.45
$2t_{1u}$	−19.6	Os(p)-Up(f)	σ-antibonding	+8.3
		Valence O-2p, U-5f6d7s		
$1t_{2g}$	−12.0	Op-Ud	π-bonding	−5.7
$2e_g$	−11.6	Op-Ud	weakly σ-bonding	−1.8
$3t_{1u}$	−11.3	Op-Uf	σ-bonding	−4.4
$1t_{2u}$	−10.6	Op-Uf	π-bonding	−3.6
$3a_{1g}$	−9.2	Op-Us	σ-antibonding	+4.1
$1t_{1g}$	−8.6	Op	π-nonbonding	+0.25
		Virtual		
$4t_{1u}$	−7.0	Op-Ufp	σ−π-antibonding	+6.9

[a] SR-ZORA/PW91/TZ2P. [b] Orbital energies ϵ in eV. [c] Variation of ϵ with U−O bond length R, dϵ/dR, in eV/Å from numerical differentiation.

Figure 1 presents DFT orbital energy level schemes for F, O, U and O_h-UX_6 (X = O, F). The MOs of UO_6 are characterized in Table 1. The well-known electronic structure of $U^{6+}F^-_6$ helps to understand the related one of UO_6.[12,18k,29d,43] The closed *semicore* shells of U-$6p^6$ and O-$2s^2$ are close in energy and interact more strongly than in UF_6, resulting in the broad set of occupied $1t_{1u}$-$1e_g$-$2a_{1g}$-$2t_{1u}$ shells. The large U-6p SO splitting[23] of nearly 10 eV transfers into the two t_{1u} shells.

TABLE 2: Formal U-5f^0 and U-5f^2 States of O_h-UO$_6$[a]

	ΔE	R(U−O)	MBO	$+q$(U)	vU-6p	U-5f	U-6d	U-7s
5f^0: NR	-0-	180.6	1.73	0.206	4.11	4.29	1.70	1.82
SR	-0-	182.0	1.54	0.561	4.84	3.14	1.78	1.85
SR+SO	-0-	182.5	1.52	0.571	4.86	3.10	1.78	1.86
5f^2: NR	−73	165.7	1.88	0.114	3.10	5.31	1.57	1.25
SR	+227	177.7	1.47	0.267	4.32	4.15	1.54	1.76
SR+SO	+204	187.7	1.21	0.226	4.78	3.79	1.49	1.87

[a] ADF/PW91/TZ2P calculations. ΔE = energy (in kcal/mol) with respect to the 5f^0 ground state; R(U−O) = bond length (in pm); MBO = Mayer U−O bond order; q(U) = Voronoi partial charge on the U atom; U-nl = Mulliken AO populations.

As pointed out earlier,[22a] it is mainly the upper U-6p$_{3/2}$ that participates in orbital interaction. The mixing in of higher valence O-2p and U-5f6d (and even a little diffuse 7s) moderates the expected U-6p^6/O-2s^2 closed-shell repulsion and thereby contributes to binding ("semicore shell binding"). This synergic interaction of semicore and valence shells had also been mentioned earlier.[25] It withdraws electron density from the U-6p semicore shell and causes the "6p core hole oxidation" which is coupled to 6p-5f-6d hybridization and ligand interaction. The orbital population values in Table 2 show the substantial U-6p vacancy of more than 1e. The 6p$_{3/2}$-hole leads to a slight relativistic bond expansion,[24] here of about 2 pm (1.4 pm by scalar relativity and 0.5 pm by SO coupling). Similar expansions are also known for organo-actinide complexes,[44] while larger relativistic bond contractions are much more common.[45,46]

The X-2p and U-5f,6d,7s *valence shells* contribute 36 (F) or 30 electrons (O). The six X-2p σ orbitals give rise to MOs 2e$_g$ (stabilized by U-6d), 3t$_{1u}$ (stabilized by U-5f) and 3a$_{1g}$ (the U-7s being rather ineffective, Figure 2 right), see Table 1. The energy ordering 2e$_g$ < 3t$_{1u}$ < 3a$_{1g}$ is consistent with the order of the uranium AO radii (see above) and with the order of the overlaps of the oxygen valence shells with {U-6d: U-6p: U-5f: adjacent O-2s2p} being approximately {0.3 : 0.2 : 0.14 : 0.1}. Because SO splitting is more than an order of magnitude less for U-5f than for U-6p, the 3t$_{1u}$ is only marginally split. The 12 electrons in the 2e$_g$, 3t$_{1u}$, 3a$_{1g}$ shells represent U^{6+} ← X$^-$ dative polar σ-bonds, although only of 2/3 bond order, since a$_{1g}$ is not bonding.

The 12 X-2p π-*type* orbitals give rise to 1t$_{2g}$, 1t$_{2u}$, 1t$_{1g}$, 4t$_{1u}$ MOs, where 1t$_{2g}$ is strongly stabilized by U-6d, 1t$_{2u}$ by U-5f, and the 1t$_{1g}$ remains nonbonding (the HOMO, Figure 2 middle), see Table 1. Especially noteworthy is 4t$_{1u}$, which is of mixed $\sigma-\pi$ antibonding type (U(f+p) − X(p$\sigma+\pi$), see Figure 2 left. This t$_{1u}$ again exhibits a remarkable SO splitting due to the U-6p admixture (Figure 1). In UF$_6$, the F-2pπ type orbitals are fully occupied and give rise to strongly polarized U^{6+} ← F$^-$ dative π-bonds, of 1/2 bond order. They are usually characterized as being ionic due to the large difference in electronegativity. The length of the U ← F $\sigma+\pi$ bonds is 200 pm, corresponding to a total $\sigma-\pi$ bond order of 1.8 according to Pyykkö's single−double-triple-bond radii.[20]

In the case of UO$_6$, there are 6 electrons less so that the U-5f − O-2p antibonding 4t$_{1u}$* MO remains empty. The U−X bond order in UO$_6$ is thus larger than in UF$_6$ by 1/2. However, since nuclear charge and number of electrons are simultaneously smaller in O than in F, similar charge distributions are expected for U^{6+}F$^-_6$ and UO$_6$. *The oxygen atoms in UO$_6$ will exhibit less tendency to form the ubiquitous closed-shell O^{2-} ligands*. Previous calculations of UO$_6$ with spin-averaged effective core potentials gave optimized U−O bond distances of 173.3 pm (DF, SCF typically yielding short values), 181.8 pm (MP2) and 174.3 pm (MRCI + Q).[12] Our present SR and SR + SO DFT bond distances scatter around the higher MP2 value (∼181 pm, see Table S1 in the Supporting Information). Interpolation of Pyykkö's bond radii yields a bond order of 2.35, corresponding to the above-mentioned estimates of (2/3 + 1/2 + 1/2 + semicore contribution). The U−O bond in UO$_6$ is about 10 pm longer than the one in uranyl, [UO$_2$]$^{2+}$, which is usually counted as a U≡O triple bond. The latter corresponds to Pyykkö's triple-bond length of 171 pm. One may also argue that U−O in UO$_6$ is longer than the axial bonds of uranyl, since O_h-UO$_6$ is more crowded than the common uranyl complexes [UO$_2$L$_{4-6}$]$^{2+}$. Namely, the equatorial oxo-ligands L are typically bound at extended single-bond distances of 2.4−2.5 Å, whereas the four "equatorial" oxygen atoms in UO$_6$ are bound at the same short distance of 1.8 Å.

U^{6+}(F$^-$)$_6$ is a closed-shell species with a HOMO−LUMO Kohn−Sham energy-gap around 2.6 eV (the experimental gap from electronic excitation is 3.1 eV).[47] The 4t$_{1u}$ (g$_{3/2u}$) HOMO is dominantly F-2p, and the 1a$_{2u}$ (e$_{5/2u}$) LUMO is dominantly U-5f. In contrast, the isostructural UO$_6$ has a much smaller gap of only 0.9 eV (Figure 1) between the O-2p type 1t$_{1g}$ (g$_{3/2g}$) HOMO and the now unoccupied spin−orbit split 4t$_{1u}$* (e$_{1/2u}$) LUMO of {O-2p − U-5f6p} character. Since the 4t$_{1u}$* LUMO is U−O antibonding, formation of high-spin UO$_6$ multiradicals is energetically not beneficial. Our calculations show that the unpaired oxygen spins of the six individual O atoms are coupled into "Lewis electron pairs" through U−O and weak O−O orbital overlap, leading to a stable singlet ^1O_h-UO$_6$ structure. However, slight geometric deformation of the octahedral complex could cause frontier orbital mixing, which might lead to higher spin states and/or to O−O triplet bonding. The natural question arises: Is the octahedral ^{1}A$_{1g}$ state of UO$_6$ stable against second-order or pseudo Jahn−Teller geometric distortions linked with electronic deformations?

Calculated vibrational frequencies with various relativistic approximations, DFT methods and basis sets are collected in the Supporting Information (Table S1). The indirect relativistic push-up of the U-5f and U-6d orbitals[23,48] stabilizes the O_h

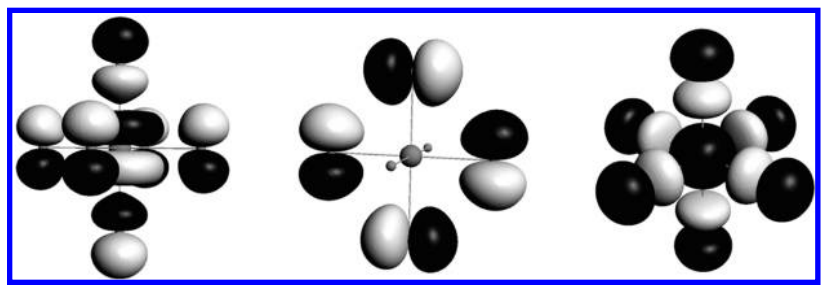

Figure 2. Frontier orbitals of ^1O_h-UO$_6$. Left: One of the antibonding 4t$_{1u}$* σ/π-LUMO {U-p,f(26%) − O(1,2)pσ(29%), O(3,4,5,6)pπ(45%)}. Middle: One of the nonbonding 1t$_{1g}$ π-HOMO {U(0%); O(1,2)(0%); O(3,4,5,6)pπ(100%)}. Right: The antibonding 3a$_{1g}$* σ-HOMO-1 {U-s(4%) − O(1,2,3,4,5,6)pσ(96%)}.

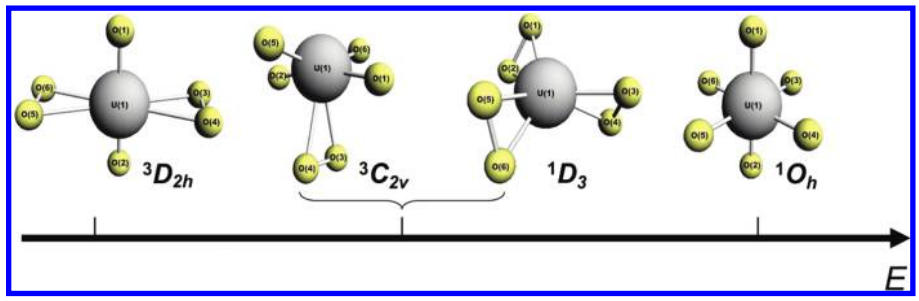

Figure 3. UO_6 isomers, from left to right: low-energy $^3D_{2h}$-$UO_2(O_2)_2$; $^3C_{2v}$-$UO_4(O_2)$ and $^1D_3$-$U(O_2)_3$ at intermediate energies; high-energy ^1O_h-UO_6.

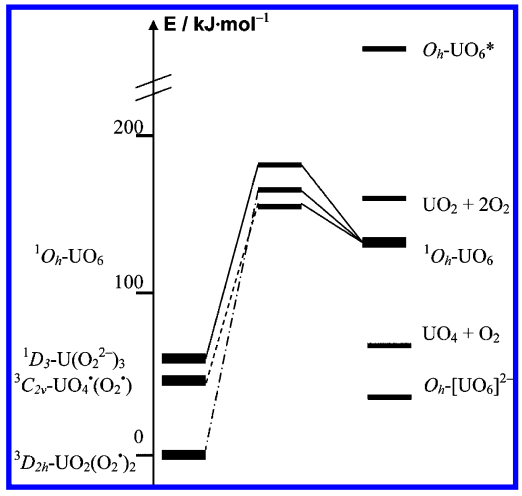

Figure 4. Relative energies of various (U+6O) species including: right side - ^1O_h-UO_6, ^1O_h-UO_6^{2-} and ^3O_h-UO_6* with formal U-5f^2 configuration; left side - $^1D_3$-$U(O_2^{2-})_3$, $^3C_{2v}$-$UO_4(O_2^{-})$, $^3D_{2h}$-$UO_2(O_2^{-})_2$; middle - some of the estimated transition states.

symmetry at the SR and SR + SO levels, all vibrational frequencies becoming real. Applying common DFT scaling-factors for lighter atomic systems,[49] we predict IR active T_{1u} stretching and bending modes near 770 and 330 cm^{-1}; Raman active A_{1g} and E_g stretching modes around 750−700 cm^{-1} and a T_{2g} bending mode near 350 cm^{-1}; and a soft T_{2u} bending mode near 200 cm^{-1}. The respective U−O bond force constant is about 5.5 N/cm, as expected being slightly stronger than the U−F one of UF_6 (4.7 N/cm).

Because of the small energy gap between the HOMOs ($3e_{1/2g}$, $4e_{1/2g}$, $4g_{3/2g}$) and the LUMO ($4e_{1/2u}$), low-lying states with different orbital occupation and spin coupling are to be expected.[12] An alternative configuration with a lower U-6p semicore population and a higher U-5f valence population has a low energy at the nonrelativistic level, but is shifted 12 eV up by relativity (Table 2).

The low energy of the above-mentioned t_{1u} ($e_{1/2u}$) LUMO (Figures 1 and 2) led Pyykkö et al. to suggest the "less oxidized" $[UO_6]^{2-}$ dianion. This is supported by our preliminary ADF/SR + SO/PW91 calculations. $[UO_6]^{2-}$ might become stabilized by bulky cations in the condensed phase. The U−O distance is enlarged to 192.1 pm, that is, by about 10 pm wrt neutral UO_6.

4. Isomers of UO_6

Since the O-2p shells in O_h-UO_6 are not fully occupied, we may expect the O atoms to have some free valence so that O···O distance reduction may lead to O−O bond formation and some energy gain. By optimizing the system of one U and six O atoms with different starting geometries we found, in addition to the hexa-oxo complex $^1A_{1g}$-O_h-$U(O)_6$, three stable species with 1, 2, or 3 dioxido ligands: $^3B_2$-C_{2v}-$U(O)_4(O_2)$, $^3B_{3u}$-D_{2h}-$U(O)_2(O_2)_2$ and $^1A_1$-D_3-$U(O_2)_3$, respectively (Figures 3 and 4). The optimized U−O and O−O distances, uranium Voronoi and Weinhold partial charges qV(U) and qW(U), U−O bond orders (MBO and WBO) and Mulliken overlap populations (MOP) are listed in Table 3.

The dioxido ligands in $U(O)_4(O_2)$ and $U(O)_2(O_2)_2$ have short O−O bond lengths at 127−131 pm, corresponding to slightly contracted O_2^{1-}. On the other hand, the dioxido ligands in $U(O_2)_3$ have O−O bond lengths at 144 pm, similar to the ones of crystalline peroxides. The slight "contraction" of O_2^{2-} may indicate the donation of some O_2-π* density to the central U cation. We may expect that O_2^{2-} is a better dative bond donor with stronger ionic attraction to the U central cation than O_2^{-}.

TABLE 3: Calculated Properties of Various UX_n Species (X = O, F)[a]

isomers	figure	qV(U)/qW(U)	U-X(1)	MBO_{U1}/WBO_{U1}	U-X(5)	MBO_{U5}/WBO_{U5}	U-X(3)	MBO_{U3}/WBO_{U3}	X(3)-X(4)	MOP_{34}
$^1A_{1g}$-O_h	3a	0.56	182.0	1.54	182.0	1.54	182.0	1.54	257.4	0.02
UO_6		1.95	[182.5]	1.45	[182.5]	1.45	[182.5]	1.45	[258.1]	
$^3B_2$-C_{2v}	3b	0.48	183.0	1.79	184.0	1.73	239.8	0.42	126.5	0.39
$UO_4(O_2)$		2.40	[182.7]	1.49	[183.3]	1.46	[238.8]	0.37	[127.0]	
$^3B_{3u}$-D_{2h}	3c	0.53	179.3	2.11	235.6	0.54	235.6	0.54	131.3	0.30
$UO_2(O_2)_2$		2.61	[179.4]	1.65	[235.0]	0.39	[235.0]	0.39	[131.2]	
$^1A_1$-D_3	3d	0.48	209.7	1.06	209.7	1.06	209.7	1.06	143.7	0.20
$U(O_2)_3$		2.52	[209.3]	0.89	[209.3]	0.89	[209.3]	0.89	[144.0]	
$^1A_{1g}$-O_h	~3a	0.49	200	0.78	200	0.78	200	0.78	283	−
UF_6		−	−	−	−	−	−	−	−	
$^1\Sigma_g^+$-$D_{\infty h}$		1.53	172	2.60	−	−	−	−	−	−
UO_2^{2+}		−	−	−						

[a] qV(U): Voronoi (2nd entries qW(U): Weinhold) charges on U; U−X and X−X: internuclear distances in pm, for the serial numbers of the O atoms in parentheses see Figure 3; MBO (WBO): Mayer (2nd entries: Wiberg) bond orders for U−X; MOP: Mulliken overlap populations for O−O. − Calculated with PW91/TZ2P/ADF for SR [SR+SO in brackets] optimized geometries, the second entries with PW91/SDD+2G, aug-cc-pVTZ/G03 at the ADF-SR optimized geometries.

TABLE 4: Calculated Relative Energies (in kcal/mol) of UO_6 Isomers[a]

rel/XC/basis/program	^1O_h-UO_6	$^1D_3$-$U(O_2)_3$	$^3C_{2v}$-$UO_4^{\bullet}(O_2^{\bullet})$	$^3D_{2h}$-$UO_2(O_2^{\bullet})_2$
spin-(un)paired closed (or open) shell	closed	closed	open	open
SR[+SO]/PW91/TZ2P/ADF	91 [88]	43 [41]	27 [17]	-0-
SR[+SO]/PW91/VTZpol/NWChem	90 [86]	43 [41]	26 [14]	-0-
SR[+SO]/B3LYP/VTZpol/NWChem	152 [148]	59 [56]	[b][b]	-0-
SR[+SO]/M06/VTZpol/NWChem	139	69	49	-0-
SR/CCSD(T)/VTZpol/NWChem	132	58	54	-0-

[a] Calculated at the SR [in brackets: SR+SO] levels, with different XC functionals, basis sets and programs. VTZpol means RSC+2g basis on U and AVTZ basis on O. [b] Serious physical spin state mixing.

The respective O−O MOPs of 0.4 and 0.2 support our assignments. The U−O distances of O_2^- are around 235−240 pm, with MBOs at 0.5 (corresponding to U−O single bonds). On the other hand, the U−O distances of O_2^{2-} in $U(O_2)_3$ are only at 210 pm, with MBOs at 1.0. The latter corresponds to U−O double bonds, to be compared with MBO ∼0.8 for U═F in O_h-UF_6 with F^- ligands at similar bond length and strength.[43]

All mono-oxido uranium distances are around 182 (±2) pm, corresponding to a reduced triple bond; the MBOs are in the range of 1.5−1.8. The Voronoi and Hirshfeld partial charges of the UO_6 isomers and of UF_6 vary by ±8%, the Weinhold, Bader and ESCA-type charges vary somewhat more. However, the trends among these molecules are not consistent. The uncertainty and "statistical noise" in all the dozens of physical charge definitions are well documented.[2] So we get only the qualitative indication of roughly similar charges in UF_6 and the isomers of UO_6, indicating similar bonding of F^- and O^{q-}. The partial charge on U in "naked uranyl", $[U^{6+}(O^{2-})_2]^{2+}$, is significantly higher than in the UO_6 species.

In the two spin-triplet species, $[U(O)_4]^{\bullet}(O_2^{\bullet})$ and $[U(O)_2](O_2^{\bullet})_2$ (the latter being the energetically lowest isomer), about one unit of unpaired spin density sits on the $(O_2^{\bullet})^-$ units. In the $[U(O)_4]^{\bullet}$ group, about one spin unit is distributed over the five atoms. Both UO_6 species form diradicals. As before, SO coupling shows little influence on the molecular geometries.[44] However, it does affect the relative energies of the four UO_6 isomers to a certain extent (Table 4). The most significant SO change in relative energies occurs to the $^3B_2$-C_{2v}-$UO_4(O_2)$ structure, due to the U-6p admixture of one of its singly occupied MOs.

Because O_h-UO_6 is by far highest in energy, we need to locate the transition states and estimate the activation barriers of the pathways to the lower isomers. For a first qualitative survey, we chose the linear synchronous transit (LST) approach in the projected crossing region of various singlet, triplet, quintet, and septet potential energy surfaces (PES) with the help of the fractional occupation number (FON) DFT-formalism for multiconfigurational spin-flip problems at the SR-PW91/TZ2P level.[36] The singlet and triplet reaction paths for converting the ^1O_h structure to the second lowest $^3C_{2v}$ structure are displayed in Figure 5, where we have not plotted the higher (quintet and septet) spin states at the top of the transition region. The isomerization processes are obviously highly multiconfigurational. Three isomerization transformations from O_h to D_3, C_{2v} and D_{2h} were investigated and the approximately estimated energy barriers are sketched in Figure 4. It remains an open question, whether O_h-UO_6 can exist as a kinetic product, amid the thermodynamic reality that dissociation processes such as $UO_6 \rightarrow UO_2 + 2O_2$ are endothermic. The other isomers may be kinetically more stable and easier to detect experimentally.

Preliminary SR/ADF/PW91/TZ2P calculations show (Table 5) that the vibrational spectroscopic fingerprints of the four UO_6 molecular species are qualitatively different enough to characterize them easily by IR and Raman spectra, if some noble gas

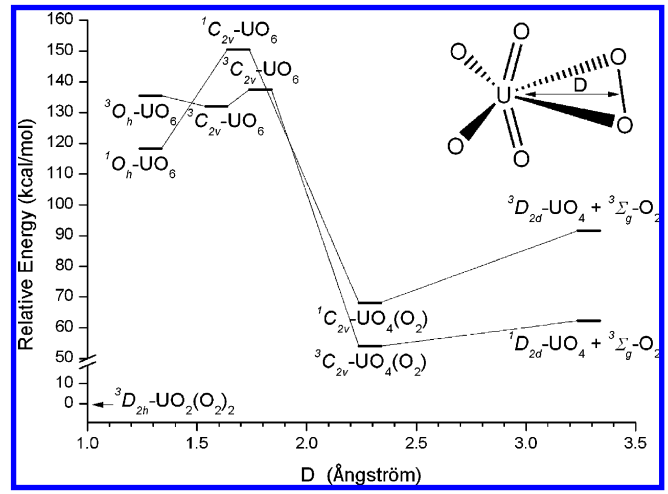

Figure 5. FON-LST reaction paths (energies in kcal/mol) for one pair of O atoms leaving ^1O_h-UO_6, vs the U−O_2 distance D (in Å), to form $^{1,3}C_{2v}$-$UO_4(O_2)$ and the dissociation products $^{1,3}D_{2d}$-UO_4 + $^3\Sigma_g^-$ O_2. The energy zero refers to the $^3D_{2h}$-$UO_2(O_2)_2$ ground state.

matrix deposition material contains UO_n molecules. Our predictions are: ^1O_h has one strong IR band around 800 (U−O_6 stretch); $^1D_3$-$U(O_2^{2-})_3$ has one strong IR band around 900 (O−O stretch), and two medium ones around 500; $^3D_{2h}$-$UO_2(O_2^-)_2$ has two strong IR bands around 1200 (O−O stretch) and 900 (O−U−O stretch), and one medium below 400 ($O_2 > U < O_2$ stretch); and $^3C_{2v}$-$UO_4(O_2^-)$ has a strong IR band around 1300 (O−O stretch) and a pair around 800 (O−U−O stretches).

5. Conclusions and Outlook

The early seventh-row elements have a dense band of many *lj* valence levels participating in covalent interactions. In addition, the Rn noble gas shell is no longer that noble. Both result in unusual chemical behavior. Furthermore, oxygen ligands occur in various bonding and oxidation states. We have investigated a whole manifold of metastable UO_6 species. All of them have very small frontier-orbital energy gaps and require further extended *ab initio* multireference descriptions at the relativistic spin−orbit coupled level. Our approximately correlated SR + SO DFT and single-reference SR-CCSD(T) calculations support the existence of hexaoxo-uranium $^1A_{1g}$-O_h-$U(O)_6$ as a local minimum on the energy surface. However, this UO_6 is far from competitive in energy with its lower-symmetry isomers, which may be more likely to be identified under appropriate experimental conditions, for example, in low-temperature inert-gas matrices.[27]

The closed-shell triperoxido-uranium $^1A_1$-D_3-$U(O_2^{2-})_3$ and the diradical triplet tetraoxo-superoxido-uranium $^3B_2$-C_{2v}-$UO_4^{\bullet}(O_2^{\bullet})_1$ are less labile isomers than $^1A_{1g}$-O_h-$U(O)_6$, whereas the diradical dioxo-disuperoxido-uranium $^3B_{3u}$-D_{2h}-$UO_2(O_2^{\bullet})_2$ is at the lowest energy. So far, only peroxido-uranyl compounds are experimentally known with long O−O

TABLE 5: Vibrational Frequencies of the Four UO_6 Isomeres[a]

energy range	^1O_h-UO_6	$^3C_{2v}$-$UO_4^{\bullet}$ ($O_2^{\bullet}$)	$^3D_{2h}$-UO_2 ($O_2^{\bullet}$)$_2$	$^1D_3$-U (O_2^{2-})$_3$
1300−1100		**1302** A_1 (IR,R) $I = 175$	1201 A_g (R)	
			1187 B_{3u} (IR) $I = 163$	
925−875			**927** B_{1u} (IR) $I = 326$	940 A_1 (R)
				915 E (IR,R) $I = 311$
825−700	**806** T_{1u} (IR) $I = 274$	**814** B_2 (IR,R) $I = 111$	845 A_g (R)	
	744 A_{1g} (R)	**786** B_1 (IR,R) $I = 125$		
	723 E_g (R)	755 A_1 (IR,R) $I = 22$		
675−625		663 A_1 (IR,R) $I = 5$		
525−450				*522* E (IR,R) $I = 58$
				516 A_1 (R)
				514 A_2 (IR) $I = 21$
				479 E (IR,R) $I = 48$
450−400		438 B_2 (IR,R) I∼0		
400−325	353 T_{2g} (R)		394 B_{2u} (IR) $I = 5$	
	339 T_{1u} (IR) $I = 13$		*390* B_{3u} (IR) $I = 72$	
			380 B_{1g} (R)	
			358 A_g (R)	
300−150	207 T_{2u}	293 A_1 (IR,R) $I = 2$	237 B_{3u} (IR) $I = 7$	197 A_1 (R)
		292 B_1 (IR,R) $I = 6$	207 B_{2g} (R)	
		262 A_1 (IR,R) $I = 21$	200 B_{3g} (R)	
		258 B_2 (IR,R) $I = 4$	178 A_u	
		217 A_1 (IR,R) I∼0	165 B_{2u} (IR) $I = 24$	
		220 A_2 (R)		
		192 B_1 (IR,R) I∼0		
<150		132 B_2 (IR,R) I∼0	118 B_{1u} (IR) $I = 3$	142 E (IR,R) $I = 4$
		104 A_2 (R)	7 B_{2u} (IR) $I = 4$	95 E (IR,R) $I = 19$
				71 A_2 (IR) $I = 26$

[a] SR/ADF/PW91/TZ2P calculations, frequencies in cm^{-1} (values may be a few % too high). IR means infrared active (absorption intensity I in km/mol; heavy bold face numbers indicate the strong IR lines, italic ones are the medium strong lines); R means Raman active.

distances (∼1.5 Å) and low O−O frequencies (∼800 cm^{-1}). We predict superoxido species with shorter O−O bonds (∼1.3 Å) and higher O−O frequencies (up to 1200 cm^{-1}), see also ref 28. The lighter homologue $CrO_2(O_2^{\bullet})_2$ of D_{2h}-$UO_2(O_2^{\bullet})_2$ has recently been identified by the noble-gas matrix-isolation technique.[27] The spin-coupling of the open-shell ligands (such as $O^{\bullet-}$, $O_2^{\bullet-}$, and $O_3^{\bullet-}$) is mediated by the uranium valence shell to an extent that is just at the borderline between ground state singlets and multiplets. The DFT approximation may not be reliable enough to guarantee the triplet character of the D_{2h} ground state.

UF_6 is a closed-shell species with closed-shell F^- ligands. In the various UO_6 species, we meet monoxido ligands that have nonclosed O-2p shells and are better described by less common monovalent O^- than by O^{2-}. In contrast to F^-, the O^- orbital levels are nearer in energy to those of the U central ion (Figure 1). The O-2s semicore shell strongly interacts with the U-6p semicore shell, resulting in U-6p vacancies that partially fill up the O-2p vacancy. On the other hand, the overlap of the O-2p valence shells with uranium partially occupies the U-5f6d valence shells. This is to be interpreted as U(d,f)-O(p) $\sigma-\pi$-covalence, not as U-f^n of lower oxidation state than +6. Any integer oxidation state such as U^{6+}, O^{1-}, or even O_2^{1-} does not fully account for the complexity of the actinoids' valence shell. This is another point than the "indirect" relation of oxidation state and "effective atomic charge". The specification of effective charges on uranium, and consequently also on the oxygens, pose a fuzzy problem. Future bond energy and charge density partitionings must uncover whether the contribution from "core shell binding" is large enough to require a "downward valence expansion" including the U-6p shell so as to obtain chemically sensible uranium oxidation state larger than +6, or even larger than +8. In view of the stability of U-$6p_{1/2}$, the highest oxidation state of U could at most be +10.[13]

The coordination number of U in uranyl complexes varies between 6 and 8. [UO_8] units occur in various polyoxo-uranate crystals. Figure 3 suggests the addition of O or η^1-O_2 or η^2-O_2 or η^2-O_3 in various charge states to some of the UO_6 species. The UO_n chemistry is an open field for further theoretical and experimental research.

Acknowledgment. The authors dedicate this work to the still active doyen in the field of chemical bonding, Professor Klaus Ruedenberg, on the occasion of his 90th birthday. They are grateful to Professor Pekka Pyykkö for helpful discussion. This work was supported by NKBRSF (2007CB815200) and NSFC (20525104, 20933003) of China. The calculations were partially performed using the Magic Cube cluster at Shanghai Supercomputer Center and the DeepComp 7000 Supercomputer at the Computer Network Information Center, Chinese Academy of Sciences. W.H.E.S. thanks for the hospitality he is receiving at Tsinghua University.

Supporting Information Available: Cartesian coordinates of the isomers and reaction paths and vibrational frequencies are available free of charge via the Internet at http://pubs.acs.org.

References and Notes

(1) (a) Frenking, G.; Shaik, S., Eds.; *J. Comput. Chem.* **2007**, *28* (1−2). (b) Poater, J.; Solà, M.; Bickelhaupt, F. M. *Chem.−Eur. J.* **2006**, *12*, 2889, 2902. (c) Bader, R. F. W. *Chem.−Eur. J.* **2006**, *12*, 2896. (d) Bader, R. F. W. *Chem.−Eur. J.* **2005**, *11*, 1. (e) Bader, R. F. W. *J. Phys. Chem A* **2009**, *113*, 10391. (f) Bitter, T.; Wang, S. G.; Ruedenberg, K.; Schwarz, W. H. E. *Theor. Chem. Acc.* **2010**, *127*, online May 21. (g) Wang, S. G.; Qiu, Y. X.; Schwarz, W. H. E. *Chem. Eur. J.* **2010**, *16*, in press.

(2) Meister, J.; Schwarz, W. H. E. *J. Phys. Chem.* **1994**, *98*, 8245.

(3) (a) Riedel, S.; Kaupp, M. *Coord. Chem. Rev.* **2009**, *253*, 606. (b) Gong, Y.; Zhou, M. F.; Kaupp, M.; Riedel, S. *Angew. Chem., Int. Ed.* **2009**, *48*, 7879. (c) Schulz, A.; Liebman, J. F. *Struct. Chem.* **2008**, *19*, 633. (d) Kemsley, J. N. *Chem. Eng. News* **2007**, *85* (33), 17.

(4) (a) Alvarez, S.; Hoffmann, R.; Mealli, C. *Chem.—Eur. J.* **2009**, *15*, 8358. (b) Aullón, G.; Alvarez, S. *Theor. Chem. Acc.* **2009**, *123*, 67. (c) Ball, P. *Chem. World* **2009**, *6* (1), The Crucible. (d) Jansen, M.; Wedig, U. *Angew. Chem., Int. Ed.* **2008**, *47*, 10026. (e) Resta, R. *Nature* **2008**, *453*, 735. (f) Raebiger, H.; Lany, S.; Zunger, A. *Nature* **2008**, *453*, 763. (g) Guerra, C. F.; Handgraaf, J. W.; Baerends, E. J.; Bickelhaupt, F. M. *J. Comput. Chem.* **2004**, *25*, 189.

(5) (a) McNaught, A. D.; Wilkinson, A. *The Gold Book: Compendium of Chemical Terminology*; Blackwell: Oxford GB, 1997. (b) IUPAC Gold Book; http://goldbook.iupac.org, 2005−2009. (c) Connelly, N. G.; McCleverty, J. A. *Nomenclature of Inorganic Chemistry II: Recommendations 2000*; RSC: Cambridge GB, 2001. (d) Connelly, N. G.; Hartshorn, R. M.; Damhus, T.; Hutton, A. T. *Nomenclature of Inorganic Chemistry, IUPAC Recommendations 2005*; RSC: Cambridge GB, 2005. (e) Wikipedia. http://en.wikipedia.org/.

(6) (a) Wang, X. F.; Andrews, L.; Riedel, S.; Kaupp, M. *Angew. Chem., Int. Ed.* **2007**, *46*, 8371. (b) Riedel, S.; Kaupp, M.; Pyykkö, P. *Inorg. Chem.* **2008**, *47*, 3379. (c) Rooms, J. F.; Wilson, A. V.; Harvey, I.; Bridgeman, A. J.; Young, N. A. *Phys. Chem. Chem. Phys.* **2008**, *10*, 4594. (d) Maron, L.; Dommergue, A.; Ferrari, C.; Delacour-Larose, M.; Fain, X. *Chem.—Eur. J.* **2008**, *14*, 8322.

(7) Gong, Y.; Zhou, M. F.; Kaupp, M.; Riedel, S. *Angew. Chem., Int. Ed.* **2009**, *48*, 7879.

(8) (a) Aleinikov, N. N.; Vasil'ev, G. K.; Kashtanov, S. A.; Makarov, E. F.; Chernyshev, Y. A. *Kinet. Catal.* **2003**, *44*, 16. (b) Zelenov, V. V.; Loboda, A. V.; Aparina, E. V.; Dodonov, A. F.; Aleinikov, N. N.; Kashtanov, S. A. *Chem. Phys. Rep.* **1998**, *17*, 687. (c) Gundersen, G.; Hedberg, K. *J. Chem. Phys.* **1970**, *52*, 812. (d) Huston, J. L.; Studier, M. H.; Sloth, E. N. *Science* **1964**, *143*, 1162.

(9) (a) Spitsyn, V. I.; Gelman, A. D.; Krot, N. N.; Zakharova, F. A.; Komkov, Y. A.; Shilov, V. P.; Smirnova, I. V. *J. Inorg. Nucl. Chem.* **1969**, *31*, 2733. (b) Tsushima, S. *J. Phys. Chem. B* **2008**, *112*, 13059. (c) Straka, M.; Dyall, K. G.; Pyykkö, P. *Theor. Chem. Acc.* **2001**, *106*, 393.

(10) Albrecht-Schmitt, T. E. *Angew. Chem., Int. Ed.* **2005**, *44*, 4836.

(11) (a) Capone, F.; Colle, Y.; Hiernaut, J. P.; Ronchi, C. *J. Phys. Chem. A* **1999**, *103*, 10899. (b) Parrot, R.; Boulanger, D.; Gendron, F.; Naud, C. *Phys. Rev. B* **2004**, *69*, 035112.

(12) Pyykkö, P.; Runeberg, N.; Straka, M.; Dyall, K. G. *Chem. Phys. Lett.* **2000**, *328*, 415.

(13) Walch, P.; Ellis, D. E. *J. Chem. Phys.* **1976**, *65*, 2387.

(14) Dyall, K. G. *Chem. Phys.* **2005**, *311*, 19.

(15) Hoffmann, R. *Am. Sci.* **2001**, *89*, 311.

(16) Schulz, A.; Liebman, J. F. *Struct. Chem.* **2008**, *19*, 633.

(17) (a) Huber, K. P.; Herzberg, G. *Molecular Spectra and Molecular Structure. IV. Constants of Diatomic Molecules*; Van Nostrand Reinhold: New York, 1979. (b) http://en.wikipedia.org/wiki/; Superoxide, Peroxide, Dioxygen.

(18) (a) Goff, G. S.; Brodnax, L. F.; Cisneros, M. R.; Peper, S. M.; Field, S. E.; Scott, B. L.; Runde, W. H. *Inorg. Chem.* **2008**, *47*, 1984. (b) Zehnder, R. A.; Batista, E. R.; Scott, B. L.; Peper, S. M.; Goff, G. S.; Runde, W. H. *Radiochim. Acta* **2007**, *96*, 575. (c) Unruh, D. K.; Burtner, A.; Burns, P. C. *Inorg. Chem.* **2009**, *48*, 2346. (d) Sigmon, G. E.; Weaver, B.; Kubatko, K. A.; Burns, P. C. *Inorg. Chem.* **2009**, *48*, 10907. (e) Sigmon, G. E.; Ling, J.; Unruh, D. K.; Moore-Shay, L.; Ward, M.; Weaver, B.; Burns, P. C. *J. Am. Chem. Soc.* **2009**, *131*, 16648. (f) Kubatko, K. A.; Forbes, T. Z.; Klingensmith, A. L.; Burns, P. C. *Inorg. Chem.* **2007**, *46*, 3657. (g) Krivovichev, S. V.; Burns, P. C.; Tananaev, I. G.; Myasoedov, B. F. *J. Alloys Comp.* **2007**, *444*−*445*, 457. (h) Kubatko, K. A.; Burns, P. C. *Inorg. Chem.* **2006**, *45*, 6096. (i) Mal, S. S.; Dickman, M. H.; Kortz, U. *Chem.—Eur. J.* **2008**, *14*, 9851. (j) Takao, K.; Ikeda, Y. *Acta Cryst. E* **2010**, *66*, M539–U661. (k) Straka, M.; Patzschke, M.; Pyykkö, P. *Theor. Chem. Acc.* **2003**, *109*, 332.

(19) (a) Alcock, N. W. *J. Chem. Soc. A* **1968**, 1588. (b) Hughes-Kubatko, K. A.; Helean, K. B.; Navrotsky, A.; Burns, P. C. *Science* **2003**, *302*, 1191. (c) Burns, P. C.; Hughes, K. A. *Am. Mineral.* **2003**, *88*, 1165. (d) Ostanin, S.; Zeller, P. *Phys. Rev. B* **2007**, *75*, 073101.

(20) (a) Pyykkö, P.; Riedel, S.; Patzschke, M. *Chem.—Eur. J.* **2005**, *11*, 3511. (b) Pyykkö, P.; Atsumi, M. *Chem.—Eur. J.* **2009**, *15*, 186, 12770.

(21) (a) Pyykkö, P.; Li, J.; Runeberg, N. *J. Phys. Chem.* **1994**, *98*, 4809. (b) Pyykkö, P.; Zhao, Y. F. *Inorg. Chem.* **1991**, *30*, 3787.

(22) (a) Wadt, W. R. *J. Am. Chem. Soc.* **1981**, *103*, 6053. (b) Dyall, K. G. *Mol. Phys.* **1999**, *96*, 511.

(23) Desclaux, J. P. *Atom. Data Nucl. Data Tables* **1973**, *12*, 311.

(24) Van Wezenbeek, E. M.; Baerends, E. J.; Snijders, J. G. *Theor. Chim. Acta* **1991**, *81*, 139.

(25) Tatsumi, K.; Hoffmann, R. *Inorg. Chem.* **1980**, *19*, 2656.

(26) (a) Larsson, S.; Pyykkö, P. *Chem. Phys.* **1986**, *101*, 355. (b) de Jong, W. A.; Visscher, L.; Nieuwpoort, W. C. *J. Mol. Struct. (Theochem)* **1999**, *458*, 41. (c) Lee, E. P. F.; Soldán, P.; Wright, T. G. *Inorg. Chem.* **2001**, *40*, 5979. (d) Santos, M.; Pires de Matos, A.; Marçalo, J.; Gibson, J. K.; Haire, R. G.; Tyagi, R.; Pitzer, R. M. *J. Phys. Chem. A* **2006**, *110*, 5751.

(27) Zhao, Y. Y.; Su, J.; Gong, Y.; Li, J.; Zhou, M. F. *J. Phys. Chem. A* **2008**, *112*, 8606.

(28) (a) Li, J.; Bursten, B. E.; Liang, B.; Andrews, L. *Science* **2002**, *295*, 2242. (b) Li, J.; Bursten, B. E.; Andrews, L.; Marsden, C. J. *J. Am. Chem. Soc.* **2004**, *126*, 3424. (c) Li, J.; Hu, H. S.; Lyon, J. T.; Andrews, L. *Angew. Chem., Int. Ed.* **2007**, *46*, 9045. (d) Lyon, J. T.; Hu, H.-S.; Andrews, L.; Li, J. *Proc. Natl. Acad. Sci. U.S.A.* **2007**, *104*, 18919.

(29) (a) Lüthi, H. P.; Siegbahn, P. E. M.; Almlöf, J.; Fægri, K.; Heiberg, A. *Chem. Phys. Lett.* **1984**, *111*, 1. (b) Lüthi, H. P.; Siegbahn, P. E. M.; Almlöf, J. *J. Phys. Chem.* **1985**, *89*, 2156. (c) Buijse, M. A.; Baerends, E. J. *J. Chem. Phys.* **1990**, *93*, 4129. (d) García-Hernández, M.; Lauterbach, C.; Krüger, S.; Matveev, A.; Rösch, N. *J. Comput. Chem.* **2002**, *23*, 834. (e) Clavaguéra-Sarrioa, C.; Vallet, V.; Maynau, D.; Marsden, C. J. *J. Chem. Phys.* **2004**, *121*, 5312.

(30) *ADF 2007.01, SCM*; Vrije Universiteit: Amsterdam, 2007; http://www.scm.com.

(31) Fonseca Guerra, C.; Snijders, G.; te Velde, G.; Baerends, E. J. *Theor. Chem. Acc.* **1998**, *99*, 391. (a) Te Velde, F.; Bickelhaupt, M.; van Gisbergen, S. J. A.; Fonseca Guerra, C.; Baerends, E. J.; Snijders, J. G.; Ziegler, T. *J. Comput. Chem.* **2001**, *22*, 931.

(32) High Performance Computational Chemistry Group. *NWChem, A Computational Chemistry Package for Parallel Computers, Ver. 5.0*; Pacific Northwest National Laboratory: Richland WA, 2006.

(33) (a) Slater, C. J. *Quantum Theory of Molecules and Solids*; McGraw-Hill: New York, 1974; Vol. 4. (b) Vosko, S. H.; Wilk, L.; Nusair, M. *Can. J. Phys.* **1980**, *58*, 1200.

(34) (a) Becke, A. D. *Phys. Rev. A* **1988**, *38*, 3098. (b) Lee, C.; Yang, W.; Parr, R. G. *Phys. Rev. B* **1988**, *37*, 785. (c) Perdew, J. P.; Chevary, J. A.; Vosko, S. H.; Jackson, K. A.; Pederson, M. R.; Singh, D. J.; Fiolhais, C. *Phys. Rev. B* **1992**, *46*, 6671. (d) Perdew, J. P.; Chevary, J. A.; Vosko, S. H.; Jackson, K. A.; Pederson, M. R.; Singh, D. J.; Fiolhais, C. *Phys. Rev. B* **1993**, *48*, 4978. (e) Perdew, J. P.; Burke, K.; Ernzerhof, M. *Phys. Rev. Lett.* **1996**, *77*, 3865. (f) Perdew, J. P.; Burke, K.; Ernzerhof, M. *Phys. Rev. Lett.* **1997**, *78*, 1396.

(35) (a) Boys, S. F.; Benardi, F. *Mol. Phys.* **1970**, *19*, 553. (b) van Duijneveldt, F. B.; van Duijneveldt-van de Rijdt, J. G. C. M.; van Lenthe, J. H. *Chem. Rev.* **1994**, *94*, 1873.

(36) (a) Wang, S. G.; Chen, X. Y.; Schwarz, W. H. E. *J. Chem. Phys.* **2007**, *126*, 124109. (b) Wang, S. G.; Schwarz, W. H. E. *J. Chem. Phys.* **1996**, *105*, 4641. (c) Dunlap, B. I.; Mei, W. N. *J. Chem. Phys.* **1983**, *78*, 4997.

(37) (a) Becke, A. D. *J. Chem. Phys.* **1993**, *98*, 5648. (b) Stephens, P. J.; Devlin, F. J.; Chabalowski, C. F.; Frisch, M. J. *J. Phys. Chem.* **1994**, *98*, 11623.

(38) Adamo, C.; Barone, V. *J. Chem. Phys.* **1999**, *110*, 6158.

(39) Zhao, Y.; Truhlar, D. G. *Theor. Chem. Acc.* **2008**, *120*, 215.

(40) Küchle, W.; Dolg, M.; Stoll, H.; Preuss, H. W. *J. Chem. Phys.* **1994**, *100*, 7535.

(41) Kendall, R. A.; Dunning, T. H.; Harrison, R. J. *J. Chem. Phys.* **1992**, *96*, 6796.

(42) (a) Pedersen, B. F.; Pedersen, B. *Acta Chem. Scand.* **1963**, *17*, 557. (b) Hester, R. E.; Nour, E. M. *J. Raman Spectrosc.* **1981**, *11*, 39. (c) Gutseva, G. L.; Jena, P.; Zhai, H. J.; Wang, L. S. *J. Chem. Phys.* **2001**, *115*, 7935.

(43) Xiao, H.; Li, J. *Chin. J. Struct. Chem.* **2008**, *27*, 967.

(44) (a) Li, J.; Bursten, B. E. *J. Am. Chem. Soc.* **1998**, *120*, 11456. (b) Li, J.; Bursten, B. E. In *Computational Organometallic Chemistry*; Cundari, T. R., Ed.; Dekker: New York, 2001; Ch. 14.

(45) (a) Schwarz, W. H. E. *Phys. Scr.* **1987**, *36*, 403. (b) Schwarz, W. H. E. In *The Concept of the Chemical Bond*; Maksic, Z. B., Ed.; Springer: Berlin, 1990; p 593−643.

(46) Ziegler, T.; Snijders, J. G.; Baerends, E. J. *Chem. Phys. Lett.* **1980**, *75*, 1.

(47) Lewis, W. B.; Asprey, L. B.; Jones, L. H.; McDowell, R. S.; Rabideau, S. W.; Zeltmann, A. H.; Paine, R. T. *J. Chem. Phys.* **1976**, *65*, 2707.

(48) Schwarz, E.; van Wezenbeek, E. M.; Baerends, E. J.; Snijders, J. *Phys. B* **1989**, *22*, 1515.

(49) (a) Merrick, J. P.; Moran, D.; Radom, L. *J. Phys. Chem. A* **2007**, *111*, 11683. (b) Andersson, M. P.; Uvdal, P. *J. Phys. Chem. A* **2005**, *109*, 2937. (c) Sinha, P.; Boesch, S. E.; Gu, C. M.; Wheeler, R. A.; Wilson, A. K. *J. Phys. Chem. A* **2004**, *108*, 9213. (d) Halls, M. D.; Velkovski, J.; Schlegel, H. B. *Theor. Chem. Acc.* **2001**, *105*, 413.

JP102107N